48th AIAA Aerospace Sciences Meeting Including the New Horizons Forum and Aerospace Exposition
4 - 7 January 2010, Orlando, Florida

AIAA 2010-829

A Comparison of Wind Turbine Load Statistics for Inflow Turbulence Fields based on Conventional Spectral Methods and Large Eddy Simulation

Chungwook Sim*, Lance Manuel†, and Sukanta Basu‡

Efficient spatial and temporal resolution of simulated inflow velocity fields is important in order to derive wind turbine load statistics for design. There are not many published studies that have addressed the issue of such optimal space-time resolution. This study investigates turbine extreme and fatigue load statistics for a utility-scale 5MW wind turbine. Load statistics, spectra, and time-frequency analysis representations are compared for various alternative space and time resolutions employed in inflow turbulence field simulation. Conclusions are drawn regarding adequate resolution in space of the inflow turbulence simulated on the rotor plane prior to extracting turbine load statistics. Similarly, conclusions are drawn with regard to what constitutes adequate temporal filtering to preserve turbine load statistics. This first study employs conventional Fourier-based spectral methods for simulating velocity fields for neutral atmospheric stability conditions.

In the second part of this study, large eddy simulation (LES) is employed with fairly coarse resolutions in space and time, justified on the basis of the earlier Fourier-based stochastic simulations, to again establish turbine load statistics. A comparison of extreme and fatigue load statistics is presented for the two approaches used in inflow field generation. The use of LES-generated flows to establish turbine load statistics in this manner is computationally more expensive but the study is partly justified in order to evaluate the ability of LES to be used as an alternative to the more conventional Fourier-based stochastic approaches. A more compelling reason for using LES is that for the stable boundary layer, it is not possible to generate realistic inflow velocity fields except by using LES. This study sets the stage for future turbine load computations in such stable conditions where low-level jets, large speed and direction shears across the rotor, etc. can possibly cause large turbine loads.

I. Introduction

VERY few studies to date have addressed the issue of efficiency of spatio-temporal resolution in generating inflow velocity fields for purposes of estimating accurate load statistics for today's large utility-scale wind turbines. The present study takes on this question by making use of conventional stochastic simulation of stationary Gaussian fields using Fourier methods.

We study loads on one such utility-scale wind turbine (rated at 5 MW) that has a hub height of 90 meters and a rotor diameter of 126 meters. Our interest is in determining an acceptable frequency resolution for the inflow turbulence generation so that resulting turbine load statistics (extremes and fatigue) can be predicted without loss of accuracy. Spectral filtering of the "base inflow" generated at 32 Hz sampling is applied in the frequency domain to generate samples with some intentional loss of high-frequency energy. Likewise, grid resolution on the rotor plane (which represents a square, 140 m on each side) is varied to different degrees of coarseness and loads studied following aeroelastic simulation. The dynamic characteristics of turbine loads including the flapwise bending moment at a blade root and the fore-aft tower base bending moment are studied.

*Graduate Research Assistant, School of Civil Engineering, Purdue University, West Lafayette, Indiana 47907 (formerly at the University of Texas, Austin, Texas 78712)

†Associate Professor, Dept. of Civil, Architectural, and Environmental Engineering, University of Texas, Austin, Texas 78712

‡Assistant Professor, Department of Geosciences, Texas Tech University, Lubbock, Texas 79409.

From the study of turbine load statistics based on stochastic simulation of inflow, we note that extremely fine resolution in space and time is not necessary for reasonably accurate extreme and fatigue load predictions needed for design purposes. These same coarse spatial and temporal resolutions are next also employed in studies involving the use Large Eddy Simulation (LES) for load computations. Load statistics from stochastic simulation and LES are then compared.

II. Spatio-Temporal Resolution in Stochastic Simulation

A Fourier-based stochastic turbulence simulation procedure was used to generate the "base inflow" for this study. The code, TurbSim,[1] was used to stochastically generate full spatio-temporal wind velocity fields. The Kaimal power spectral density (PSD) function was used for the turbulence generation. It can be expressed as follows:

$$\frac{f \cdot S_k(f)}{\sigma_k^2} = \frac{4f \cdot L_k/V_{hub}}{(1 + 6f \cdot L_k/V_{hub})^{5/3}} \tag{1}$$

where f represents frequency in Hz; k is an index referring to the direction of the wind velocity component (k is set equal to 1, 2, or 3 for the longitudinal, lateral, and vertical components, respectively); $S_k(f)$ is the single-sided power spectral density function for wind velocity component, k; σ_k is the standard deviation for the wind velocity component k; L_k is the integral scale parameter for wind velocity component, k; and V_{hub} is the ten-minute average hub-height longitudinal wind speed. Values for the three wind velocity component standard deviations and integral scale parameters are specified in the IEC 61400-1 guidelines.[2]

An exponential coherence function specified in the IEC 61400-1 guidelines[2] was also used in this study. This function is expressed as follows:

$$Coh(r, f) = \exp\left[-12\left((f \cdot r/V_{hub})^2 + (0.12r/L_c)^2\right)^{0.5}\right] \tag{2}$$

where the coherence function, $Coh(r, f)$, is defined as the magnitude of the complex cross-spectral density funciton of the longitudinal wind velocity component at two spatially separated points divided by the autospectrum function; r is the magnitude of the projection of the separation vector between the two points on to a plane normal to the average wind direction; and L_c is the coherence scale parameter.

The Normal Turbulence Model (NTM) with a reference turbulence intensity of 16% (corresponding to Wind Turbine Site Class A) was used to generate the inflow velocity field. Using the NTM, the power spectra, the coherence functions, and the reference turbulence intensity, full wind fields were stochastically generated on a rotor plane for the wind turbine selected. A time step of 0.03125 seconds (representing 32 Hz sampling) was used to generate the "base inflow" turbulence. Table 1 summarizes various parameters and their values used in the inflow simulation with TurbSim. These inflow fields for three different wind speeds were filtered in the frequency domain using low-pass filters with cut-off frequencies set at 16 Hz, 8 Hz, 4 Hz, 2 Hz, 1 Hz, 1/2 Hz, 1/4 Hz, and 1/8 Hz.

Table 1. Parameters and values used in inflow turbulence field simulations.

Parameters	Values
Hub height (m)	90
Rotor diameter (m)	126
Hub-height wind speed (m/s)	12, 15, 18
Base inflow sampling rate (Hz)	32
Low-pass cut-off frequency (Hz)	16, 8, 4, 2, 1, 0.5, 0.25, 0.125
Grid (y × z)	13 × 13, 11 × 11, 9 × 9
Surface roughness (m)	0.1

The rotor plane of the selected 5MW turbine model[3] with a rotor diameter of 126 m is represented in separate analyses by 13×13, 11×11, and 9 ×9 grids that cover a square area of side 140 m, centered at the rotor hub. The 5MW wind turbine model closely represents a utility-scale wind turbine that is currently

being manufactured. This model is used for our aeroelastic response simulations. The turbine is a variable-speed, collective pitch-controlled machine. Two different turbine loads are studied; these include the flapwise bending moment at a blade root (FBM) and the tower base fore-aft bending moment (TBM). Ten-minute time series of these loads are simulated using the aeroelastic simulation tool, FAST,[4] developed at NREL.

A. Filtering of Inflow Turbulence

To the base inflow (at a 32 Hz sampling rate) obtained from TurbSim, a low-pass filter was applied in the frequency domain with cut-off frequencies defined as given in Table 1.

Power spectral densities (PSDs) computed for the various filtered longitudinal wind velocity time series at hub height are presented in Fig. 1. These estimated PSDs are based on an ensemble of 15 ten-minute simulations in each case. The PSDs are shown only up to 16 Hz, the Nyquist frequency, since all the inflow time series have an identical time step of 0.03125 seconds (32 Hz). The log-log plot shows that the inflow time series, with or without the filtering, all follow Kolmogorov's -5/3 power law for scaling of turbulence in the inertial subrange. The target Kaimal power spectrum for longitudinal turbulence at hub height is also shown in Fig. 1; the simulated PSD for the unfiltered case matches the target spectrum well; it is slightly deficient in power at frequencies above around 8 Hz. As increased filtering is applied, the PSDs drop at lower and lower frequencies as expected.

B. Power Spectral Density Functions for Turbine Loads

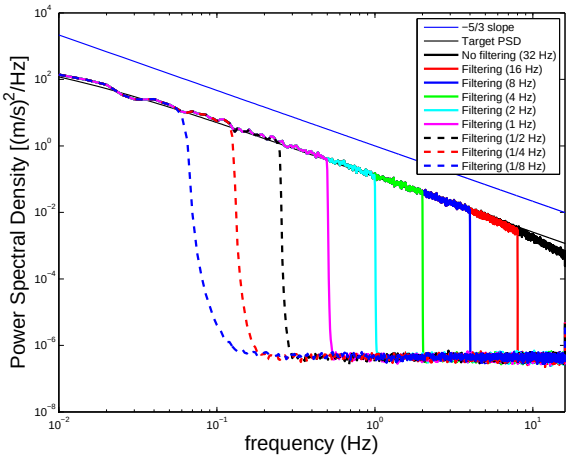

Figure 1. Target Kaimal PSD and estimated PSDs from unfiltered and filtered simulated hub-height longitudinal velocity time series.

Gravitational, inertial, and aerodynamic forces all contribute to the overall loading on wind turbine components.[5] Gravitational loading refers, for example, to the force on blades that cause periodic loading once per revolution; these forces are experienced at the rotor's rotational frequency denoted by 1P (in our case, 1P corresponds to approximately 0.2 Hz). Inertial loading is caused by acceleration or deceleration of the blade rotation, due to which, centrifugal forces are caused on the blades. This centrifugal force has two components; one is spanwise and the other is in a normal direction. These latter forces influence the flapwise bending moment (FBM) on a blade. Lastly, aerodynamic loads created by the inflow affect turbine loads. It is instructive to study power spectral density (PSD) functions of the turbine loads in order to understand the dynamic behavior of our wind turbine.

Power spectra for FBM and TBM are presented in Fig. 2. The loads data for these PSDs were generated from a full-field inflow on a 9×9 grid with hub-height ten-minute mean wind speed of 12 m/s. Because the natural modes of vibration for our wind turbine model suggest that important blade and tower vibration modes occur at frequencies below 5 Hz, log-log plots of the four PSDs were plotted only up to 5 Hz. (We note in passing that for the FAST simulation model used here, all the modes of vibration represented for the tower and blades had natural frequencies below 5 Hz. We also note that if simulation models built using other commercial codes such as ADAMS are employed, higher frequencies of vibration will likely result; however, it is our expectation that turbine loads and hence related fatigue and extreme loads are influenced only to a small degree by these higher frequencies.)

All the PSDs discussed here are estimated based on an ensemble of 15 simulations. Peaks in the PSDs due to the rotational frequencies of the blade (1P = 0.2 Hz, 2P, and 3P) and other important natural frequencies are indicated on the plots. The plots in Fig. 2 also show the PSDs derived based on filtered inflow (at various cut-off frequencies). The 1P spectral peaks and the various resonance peaks that match natural frequencies of the turbine blades and tower are easily identified and are all captured well even with filtering down to 1 Hz.

In the FBM PSD, the presence of 1P, 2P, 3P, etc. peaks is obvious; these peaks occur due to rotational sampling of the inflow turbulence by the moving blades. A 0.6 Hz peak is an indication of the first flapwise

blade bending mode. Unlike the blade loads, PSDs for the fore-aft bending moment at the tower base (TBM) in Fig. 2 show largest peaks at around 0.4 Hz (close to the 2P frequency). This frequency matches the first tower bending natural frequency.

Studying the PSDs of the tower and blade loads helps explain why tower load statistics miss the target to a greater degree than do the blade load statistics. The PSDs clearly show that the energy (related to variance which is the area under the PSD) of the blade loads is relatively concentrated to a greater degree at the low frequencies while tower loads display peaks above 2 Hz. The dominant PSD peaks for FBM are well captured by filtered inflow; TBM spectra show less dominant peaks and some deficient energy at a few spectral peaks.

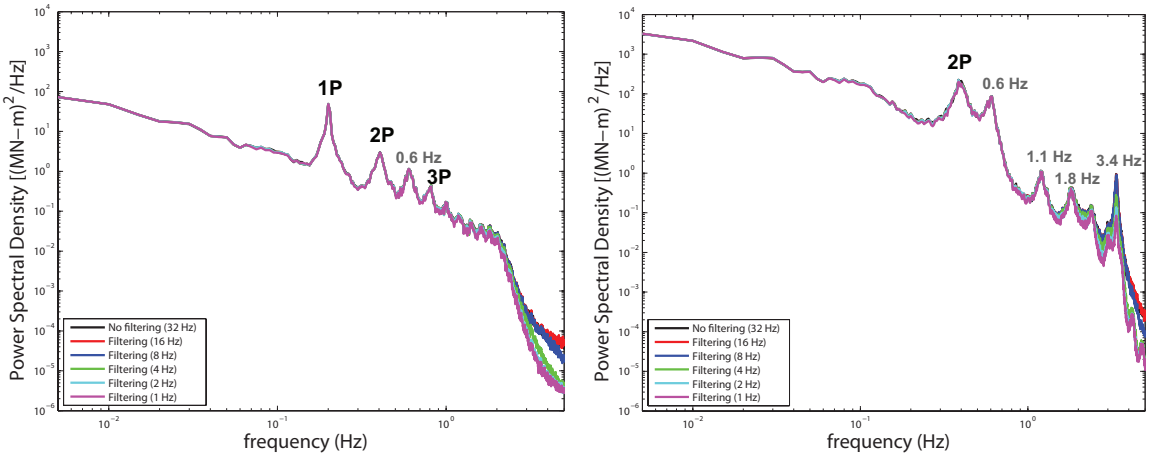

Figure 2. Power spectral density function for FBM (left) and TBM (right) from inflow simulated on a 9×9 grid and with a ten-minute mean wind speed of 12 m/s.

C. Turbine Load Statistics

We are interested in turbine load statistics for the various inflow time series generated. These inflow velocity time series are generated for (i) three different hub-height mean wind speeds (12 m/s, 15 m/s, and 18 m/s); (ii) three different spatial grids/samplings on the rotor plane (13×13, 11×11, and 9×9); and (iii) eight different filters (low-pass filters applied at 16 Hz, 8 Hz, 4 Hz, 2 Hz, 1 Hz, 1/2 Hz, 1/4 Hz, and 1/8 Hz). We estimate the standard deviation, the ten-minute extreme, and the equivalent fatigue load (EFL) for two different turbine loads (FBM and TBM). A total of fifteen simulations were used to summarize ensemble load statistics for each load for the various inflow time series. Note that for the EFL calculations, Wöhler exponents of 10 and 3 were applied for FBM and TBM, respectively.

Ensemble standard deviation estimates of the two loads studied (but not presented here) show very slight variation with hub-height mean wind speed. The various spatial grids and even the 9×9 grid with a 1 Hz filter do not lead to large errors in the load standard deviations for all load types. Ensemble ten-minute extreme load estimates show slightly decreasing trends with increase in wind speed from 12 m/s to 18 m/s. This is expected since the turbine is pitch-controlled and has rated wind speed around 11.5 m/s. Loads are reduced for wind speeds above rated due to pitching of the blades. The various spatial grids and even the 9×9 grid with a 1 Hz filter do not lead to large errors in ten-minute load extremes for all load types. Ensemble equivalent fatigue load (EFL) estimates for the loads studied show increasing trends with increase in wind speed from 12 m/s to 18 m/s. These trends with wind speed are more pronounced than for the other statistics studied—namely standard deviations and ten-minute extremes. Comparing the different spatial grids, greater variation is seen for EFL than for the other statistics. FBM EFL estimates are slightly underestimated with coarser spatial grids while EFL estimates for TBM are slightly overestimated with coarser grids (see Table 2). Still, though variation due to spatial resolution of the inflow is greater for fatigue loads, again the various spatial grids and even the 9×9 grid with a 1 Hz filter do not lead to great differences in EFL estimates for all load types.

The preceding observations suggest that it may not be necessary to employ very fine spatial sampling

while generating inflow turbulence to establish wind turbine loads for design. We conclude that a 9×9 spatial grid for our rotor may be adequate for reasonably accurate load statistics. In addition, since for all the four loads studied, the ten-minute extreme values are higher at 12 m/s wind speed than at higher wind speeds (as was also seen in a previous study[6]), further discussions on filtering will mostly focus on the inflow wind velocity time series with a mean hub-height wind speed of 12 m/s.

Table 2. Turbine load ensemble statistics (based on 15 simulations).

Grid, filtering	FBM (kN-m) 10-min extreme	FBM (kN-m) EFL	TBM (kN-m) 10-min extreme	TBM (kN-m) EFL
13 × 13, 32 Hz	12,979	5,656	82,295	12,585
9 × 9, 1 Hz (normalized)	0.985	0.949	0.983	1.011

D. Wavelet Analyses of Turbine Loads

As has been discussed by Kelley,[7] time-frequency analysis using continuous wavelet transforms can help study peaks that occur coincidentally with higher-order modes that might not be detected through spectral analysis. Wavelet analysis of the loads data was performed to determine whether cutting off high frequencies in the inflow turbulence would affect turbine load characteristics in any significant way. Also, non-stationary characteristics of loads from aeroelastic simulations such as flapwise bending loads may be lost by relying on spectral analysis.[7]

Figures 3(a),(c),(e) show results of the wavelet analysis of the flapwise bending moment (FBM) resulting from an unfiltered inflow (13×13 grid and 32 Hz sampling) and an inflow filtered at 1 Hz on a 9×9 grid (for a hub-height mean wind speed of 12 m/s). The colorbar shows FBM values in MN-m. The x-axis shows time, while the y-axis shows the time scale of the Morlet wavelet used in the analyses. At high frequencies, the time windows are narrow; while at low frequencies, the frequency windows are narrow. In other words, the long time scale "a" on the y-axis indicates low frequencies, while the short time scale indicates high frequencies.

The two wavelet plots demonstrate that there is almost no difference in the blade loads that results from filtering down to 1 Hz and using a 9×9 spatial grid for our rotor. The maximum difference in the FBM wavelet plots for the unfiltered and filtered cases is only 0.939 MN-m; peaks in time and at different scales are recovered quite well for the filtered flows.

Figures 3(b),(d),(f) show results of the wavelet analysis of the tower base fore-aft moment (TBM) for the same filtered versus unfiltered cases as were studied for FBM. The wavelet plots show that TBM derived from unfiltered and filtered inflow also do not show great differences at low frequencies, while at higher frequencies (a=2 sec) some of the peaks are missing for the filtered case.

E. Summary on Spatio-Temporal Filtering of Inflow in Stochastic Simulation

Inflow turbulence was generated based on conventional Fourier-based stochastic simulations. The base inflow was filtered with various spectral cut-off frequencies to generate inflow with different spectral content, deficient in high-frequency energy. The purpose of filtering the inflow was to evaluate whether high frequencies are actually required in aeroelastic simulations. The filtered and unfiltered inflow fields were applied as input to a 5MW wind turbine model. Turbine blade and tower load time series were studied. It was found that although power spectral density functions of the filtered inflow drop considerably with greater amounts of filtering, associated load characteristics do not change significantly. In general, for all of the loads studied, it was found that 9×9 spatial grids on the rotor plane and 1 Hz sampling could be used to estimate load statistics with reasonable accuracy. Power spectra and wavelet analyses confirmed that there was no negligible losses from such filtering.

The findings from this study suggests that a grid spacing around one-tenth of the rotor diameter (10 m) and 1 Hz inflow data may be appropriate to generate from LES to allow for comparisons with conventional stochastic simulation. Such spatial and temporal resolution of the inflow should also not lead to significant errors in load statistics.

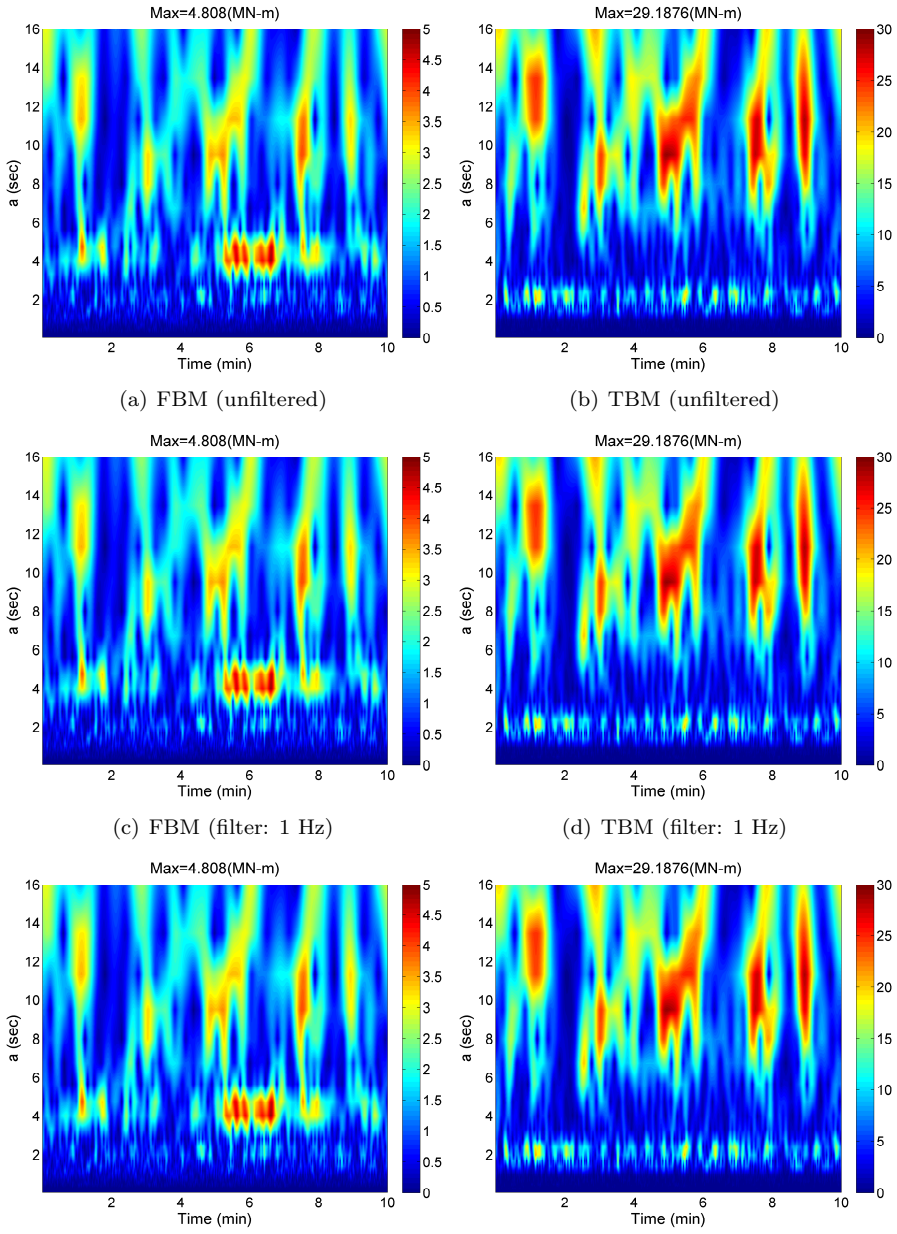

(a) FBM (unfiltered)

(b) TBM (unfiltered)

(c) FBM (filter: 1 Hz)

(d) TBM (filter: 1 Hz)

(e) Difference of FBM

(f) Difference of TBM

Figure 3. Wavelet analysis of turbine blade and tower loads

III. Large Eddy Simulation for Neutrally Stable Inflow Turbulence

Based on the preceding discussion, we determined adequate temporal and spatial sampling values that may be used for stochastic simulation of inflow wind velocity fields for wind turbine loads analysis. We assume that similar spatio-temporal resolution may be employed in large eddy simulation (LES) of inflow fields and that turbine loads based on LES and stochastic simulation may then be directly compared. While LES preserves realistic atmospheric boundary layer characteristics by directly solving the nonlinear Navier-Stokes equation and the conservation of mass equation, due to the computational effort required in such simulations, less computationally intensive stochastic simulations based on Fourier techniques are commonly used in the design of wind turbines. In contrast, however, stochastic simulations have limitations especially in modeling the stratified stable boundary layer (SBL) which is often accompanied by high wind shear and low-level jets and potentially large turbine loads. The present study is being undertaken prior to applying LES in SBL simulations; we seek first to evaluate wind turbine load statistics for ideal neutral conditions that can be simulated using stochastic techniques and compared with those based on LES-generated inflow. The theoretical background on the use of LES is summarized very briefly here. We briefly demonstrate, too, how the inflow turbulence is generated using LES with fractal interpolation which is introduced to enhance the deficient high-frequency energy.

A. Governing Equations of Large Eddy Simulation

Large eddy simulation (LES) is at present the most efficient technique available for high Reynolds number flow simulations, such as for atmospheric boundary layer (ABL) simulations, in which the larger scales of motion are resolved explicitly and the smaller ones are modeled. Over the past three decades, the field of LES for the ABL has evolved quite dramatically; LES has enabled researchers to probe various boundary layer flows by generating unprecedented high-resolution four-dimensional turbulence data. As a consequence, we have gained a better understanding of some fairly complex ABL phenomena. In rotation-influenced ABLs, the equations for the conservation of momentum (using the Boussinesq approximation) and temperature are:

$$\frac{\partial \tilde{u}_i}{\partial t} + \frac{\partial (\tilde{u}_i \tilde{u}_j)}{\partial x_j} = -\frac{\partial \tilde{p}}{\partial x_i} - \frac{\partial \tau_{ij}}{\partial x_i} + \delta_{i3} g \frac{(\tilde{\theta} - \left\langle \tilde{\theta} \right\rangle)}{\theta_0} + f_c \varepsilon_{ij3} \tilde{u}_j + F_i \tag{3}$$

$$\frac{\partial \tilde{\theta}}{\partial t} + \frac{\partial \left(\tilde{u}_j \tilde{\theta} \right)}{\partial x_j} = -\frac{\partial q_j}{\partial x_j} \tag{4}$$

where t refers to time; x_j is the spatial coordinate in the direction, j; u_j is the velocity component in the direction, j; θ is potential temperature; θ_0 is the reference surface potential temperature; p is the dynamic pressure; δ_{i3} is the Kronecker delta; ϵ_{ij3} is the alternating unit tensor; g is the gravitational acceleration; f_c is the Coriolis parameter; and F_i is a forcing term (e.g., geostrophic wind).

Molecular dissipation and diffusion are neglected here since the Reynolds number of the ABL is very high and no near-ground viscous processes are resolved. Note that $\langle . \rangle$ is used to define a horizontal plane average; also the tilde (i.e.,"$\sim$") above some variables in Eqs. 3 and 4 denotes a spatial filtering operation, using a filter of characteristic width, Δ_f. These filtered equations are now amenable to numerical solution on a grid of mesh size, Δ_g, considerably larger than the smallest scale of turbulent motion (the so-called Kolmogorov scale). The effects of the unresolved scales (smaller than Δ_f) on the evolution of $\tilde{u}_i$ and $\tilde{\theta}$ appear in the subgrid-scale (SGS) stress, τ_{ij} (in Eq. 3) and the SGS flux, q_j (in Eq. 4), respectively; these are defined as follows: $\tau_{ij} = \widetilde{u_i u_j} - \tilde{u}_i \tilde{u}_j$ and $q_j = \widetilde{u_i \theta} - \tilde{u}_i \tilde{\theta}$. Note that the SGS stress and flux quantities are unknown and must be parameterized (using a SGS model) as a function of the resolved velocity and temperature fields. Eddy viscosity models, the most popular SGS models, use the "gradient hypothesis" and formulate the SGS stress tensor (the deviatoric part) as follows:[8,9]

$$\tau_{ij} - \frac{1}{3} \tau_{kk} \delta_{ij} = -2 \nu_t \tilde{S}_{ij} \tag{5}$$

where S_{ij} is the resolved strain rate tensor and ν_t denotes the eddy viscosity.

From a dimensional analysis, ν_t can be interpreted as the product of a characteristic velocity scale and a characteristic length scale.[9] Different eddy-viscosity formulations basically use different velocity and length

scales. The most popular eddy viscosity formulation is the Smagorinsky model:[8]

$$\nu_t = (C_s \Delta_f)^2 \left| \tilde{S} \right| \tag{6}$$

where C_s is the so-called Smagorinsky coefficient, which is adjusted empirically or dynamically to account for shear, stratification, and grid resolution, and $|S_{ij}|$ is the magnitude of the resolved strain rate tensor.

Similar to the SGS stresses, eddy-diffusivity models are used for the SGS heat fluxes as follows:

$$q_i = -\nu_{ht} \frac{\partial \tilde{\theta}}{\partial x_i} = -\frac{\nu_t}{\mathrm{Pr}_{SGS}} \frac{\partial \tilde{\theta}}{\partial x_i} \tag{7}$$

where Pr_{SGS} is the SGS Prandtl number.

The values of the Smagorinsky-type SGS model parameters, C_s and Pr_{SGS}, are well established for homogeneous isotropic turbulence.[10] However, the value of C_s is expected to decrease with increasing mean shear and stratification. This expectation has been confirmed by various recent field studies. In order to account for shear and stratification, application of the traditional eddy-viscosity model in LES of ABL flows (with strong shear near the ground and temperature-driven stratification) has traditionally involved the use of various types of wall-damping functions and stability corrections, which are either based on the phenomenological theory of turbulence or empirically derived from observational data. Similarly, a priori prescriptions exist also in the case of eddy-diffusivity SGS models.

An alternative approach is to use the "dynamic" SGS modeling approach. In this approach, one computes the value of the unknown SGS coefficients (e.g., C_s in the Smagorinsky-type eddy-viscosity models) dynamically at every time and every position in the flow. By looking at the dynamics of the flow at two different resolved scales and assuming scale similarity as well as scale invariance of the model coefficient, one can optimize its value.[10,11] Thus, the dynamic model avoids the need for a priori specification and tuning of the coefficient because it is evaluated directly from the resolved scales in an LES. Recently, Basu and Porté-Agel[12] proposed a refined dynamic modeling approach (called the "locally-averaged scale-dependent dynamic" or LASDD SGS modeling approach) for ABL simulations. The potential of the LASDD SGS model was demonstrated in large-eddy simulations of the neutral boundary layer,[13] of the stable boundary layer,[12] and of a complete diurnal cycle.[14] In the present study, we utilize the LASDD model to generate neutral boundary layer inflow conditions for wind turbine load calculations using an aeroelastic model.

B. LES and Stochastic Simulation of Inflow Turbulence

In atmospheric large eddy simulations, idealized or observed soundings (i.e., 1-D vertical profiles) of wind speed and other environmental variables (such as temperature, moisture, etc.) in conjunction with small-scale 3-D perturbations (random noise) are typically used to generate initialization fields. With the help of the Navier-Stokes equations (Eq. 3), these fields are then evolved in time under the constraints of certain large-scale forcing terms (e.g., geostrophic wind) and boundary conditions (e.g., prescribed land-surface temperature is often used as the lower boundary condition). Usually, it takes about an hour of simulation (depending on the characteristics of the boundary layer to be simulated) to generate realistic turbulence (e.g., for reasonable representation of the inertial range of spectra). However, it can take a few hours of simulation to generate quasi-steady state boundary layer conditions. For realistic neutral boundary layer simulations, one needs to run an LES code for O(12) hours to reach quasi-steady state conditions.

High-resolution LES runs are computationally very expensive, especially for durations of O(12) physical hours. For this reason, in the present research study, we carry out the simulations in two phases (see Fig. 4). In Phase I, coarse runs (with a grid resolution of 20 m) of 12-hour duration are performed using a time step of 0.2 seconds. Then, in Phase II, the final 3-D fields from the phase I simulations are used as initial fields and new simulations are run for 30 minutes (with a time step of 0.1 seconds). In order to create higher resolution (finer than 20 m) LES data, we first apply a cubic spline interpolation to the final 3-D fields of the Phase I simulations to produce 13.3 m resolution initial fields. Full-field wind files for 3-D velocity components are output from the last 15 minutes of these 30-minute Phase II simulations at a frequency of 2.5 Hz (i.e., every 0.4 seconds). For both phases of our simulations, we kept a fixed domain size of 800 m $\times$ 800 m $\times$ 1,260 m.

Figure 5 shows a 180 m $\times$ 180 m (y-z plane) slice of the longitudinal velocity (U) taken at one time instant from the last 15-minute time history segment of the simulated wind field (with a grid resolution of

13.3 m); also shown are the 15-min time series for U versus vertical elevation (z) for points laterally separated by 150 m. In this study, we systematically varied geostrophic winds (a large-scale forcing term related to mesoscale pressure gradient force) to obtain various hub-height wind speeds.

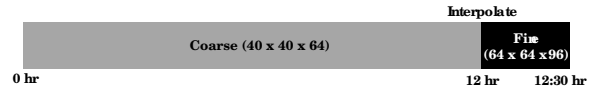

Figure 4. Two phases of the LES flow generation.

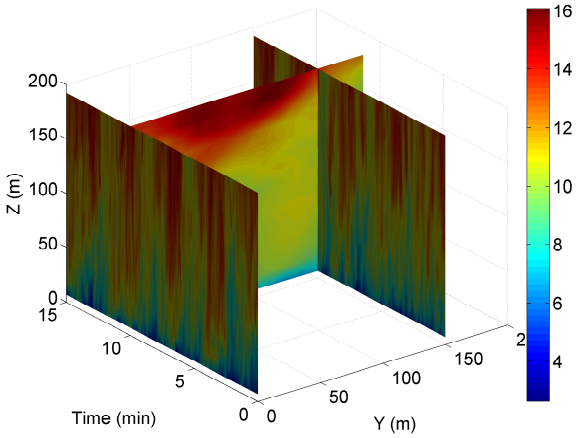

Figure 5. Slice of the last 15 minutes generated from LES: Phase II longitudinal velocity wind field

In addition, three sets of LES were generated for each geostrophic wind case. After generating these wind fields, the 800 m × 800 m × 1,260 m domain was sliced into 5 pieces in the y direction yielding a total number of 15 cases covering (lateral) rotor planes. In addition, since the w-components were generated in a staggered form vertically where they were spaced between the vertical grid points of the u and v-components, the w-components were interpolated to the grid points of u and v-components. Then, the entire turbulence field was interpolated to the same grid points that were used in generating the NBL inflow with stochastic simulations. In order to provide neutral boundary layer flows from stochastic simulations whose effects on turbine loads could be directly compared with the neutral boundary layer flows generated from LES, the Fourier-based stochastic turbulence simulation code, TurbSim, was used together with target turbulence power spectra and coherence functions (the Kaimal model). The rotor plane of the selected 5MW turbine, with a rotor diameter of 126 m, was represented as a 13 × 13 grid that covers a square area of side 160 m, centered at the rotor hub. A time-step of 0.4 seconds was used in the NBL flow simulations to match the time step from LES. Note that the resultant of u and v-component wind speed at hub height (90 m) for the LES case was matched to the hub-height mean wind speed of the TurbSim simulations. A total of 15 simulations were produced and compared with the LES results.

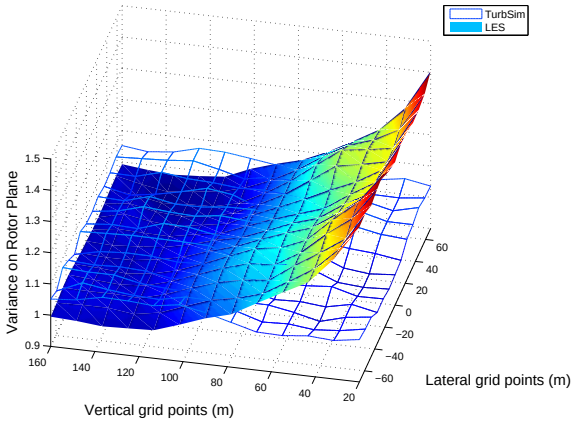

Figure 6. 3-D Variance of inflow turbulence across the rotor plane

Figure 6 shows a 3-D plot of variance of inflow turbulence across the rotor plane. The target variance in TurbSim is treated as constant over the entire rotor plane although this is not physically realistic. Large eddy simulation generates turbulence at the surface and transports it upwards in neutral flows. As a result, variance and fluxes are higher near the surface and will decrease monotonically with height. Moreover, the variance and fluxes should be zero at the top of boundary layers (BL). Figure 6 clearly demonstrates that LES is capturing the correct behavior of BL characteristics. Near the hub height (90 m) of our turbine model, the variance of LES and TurbSim match reasonably well. However, while the variance from TurbSim is constant over the entire rotor plane, the variance from LES has higher values close to the ground (20 m) and lower values above 90 m.

To evaluate the LES of neutral boundary flow (NBL) by comparing the loads from LES flows with those form TurbSim (stochastic simulator), we would like to modify any differences in inflow in reasonable ways. Though there are noted differences in inflow variance from LES versus TurbSim over the rotor plane, this

difference is preserved since LES is more realistic. A key finding from the turbulence simulation is that the inflow generated from LES is lacking in high-frequency energy while the low-frequency energy is similar to the wind field produced by TurbSim. Thus, the main area chosen for improvement is targeted at enhancing the high-frequency energy that is lacking in LES.

C. Fractal Interpolation of Large Eddy Simulations

In this study, for the large eddy simulations we used grid resolutions of O(10) m. Since spatial and (implicit) temporal filtering operations are intimately related in LES, the grid resolution basically dictated the level of high-frequency content realized in the generated time series. The LES runs with temporal frequencies of O(>2.4) Hz had minimal energy, as would be anticipated. However, in using TurbSim with the identical temporal frequency of 2.4 Hz for neutral conditions, the generated velocity time-series showed additional energy at higher frequencies. Simulation of turbulence time series with higher frequency using a large eddy model would require a grid-resolution with smaller O(0.1) m. At the present time, this is a computationally daunting task.

For such reasons, instead of performing computationally expensive high-resolution large eddy simulations, we consider the possibility of enhancing the high-frequency content of coarse-resolution LES data by using a so-called fractal interpolation technique (FIT). FIT is an iterative affine mapping procedure that may be used to construct synthetic deterministic small-scale fields from a few given large-scale interpolating points.[15] In addition, FIT is computationally very inexpensive and, more importantly, it preserves the higher-order moments and non-Gaussian probability density function of the velocity increments.[15]

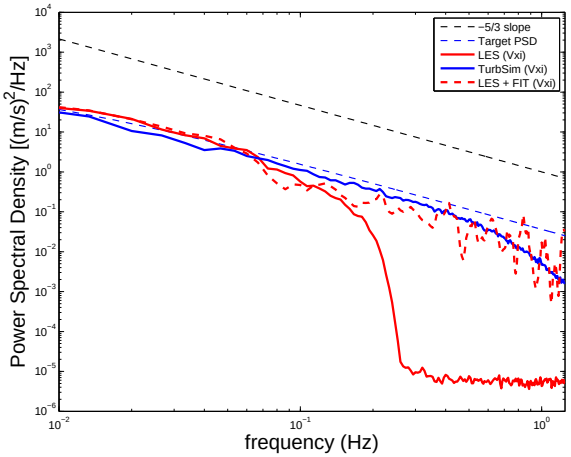

Figure 7. Power spectral densities of inflow turbulence with FIT

To evaluate FIT's capability, it is instructive to study the improvement in high-frequency energy content in the inflow by reviewing turbulence power spectral densities. The red-dotted line in Fig. 7 shows the case when FIT is applied to LES. This figure reveals that the LES-generated data can have comparable inflow turbulence to the TurbSim-generated full field by the introduction of FIT.

A goal of this study is to compare turbine loads under the influence of LES-generated wind and stochastic inflow. We have focused on the theoretically ideal (near-neutral) atmospheric boundary layer conditions. In simulating the inflow turbulence field with LES, we employed a coarse temporal resolution of 0.4 sec. In order to compare in a consistent way flows from LES and stochastic simulation and the resulting extreme and fatigue loads, the inflow turbulence of LES was modified to resolve high-frequency turbulence by employing fractal interpolation which can introduce significant portions of high-frequency energy in the inflow turbulence. Next, wind turbine loads based on LES with FIT are compared to loads using stochastic simulation.

IV. Extreme and Fatigue Wind Turbine Loads based on LES and Stochastic Simulation

We now use the inflow turbulence generated by LES and TurbSim to study turbine loads. We first study load statistics (FBM and TBM) for three different hub-height wind speeds; later, later we focus on only one wind speed (near rated) where the largest turbine loads. Power spectral densities are studied to understand dynamic characteristics of the turbine loads occurred. Then, based on the rainflow cycle-counting algorithm, fatigue stress range histograms and equivalent fatigue loads are estimated for alternative inflow turbulence fields. Finally, short-term load probability distributions of turbine load extremes are evaluated. One-minute block maxima from the time series are used to estimate short-term load distribution that can be useful in evaluating design load cases for wind turbines.

A. Turbine Load Statistics

We study turbine load statistics for the various inflow fields generated by different simulation techniques. These inflow fields are based on three different simulation models: LES, LES with FIT, and TurbSim; and three different ten-minute mean hub-height wind speeds: 12 m/s, 15 m/s, and 17 m/s. We are interested in the ten-minute extreme, the ten-minute mean, and the standard deviation for the two different turbine loads (FBM and TBM). A total of fifteen simulations were used for the turbine load calculations with each of the inflow fields. The results of these simulations are represented in box plots. These plots are also referred to as box-whisker diagrams.[16] Quartiles that represent the 25% (lower quartile), 50% (median), and the 75% (upper quartile) are extracted from the data set; these quartiles form the box. The box-whisker plots for FBM and TBM statistics illustrated in Figs. 8 and 9, respectively, identify the quartiles as well as maximum and minimum values of the relevant statistic (mean, standard deviation, or ten-minute maximum) from 15 simulations. Each figure summarizes statistics for the three inflow options (LES, LES + FIT, TurbSim) and the three wind speeds. The red box represents the LES case; the green box represents the case for LES inflow with fractal interpolation; and the blue box represents the TurbSim case.

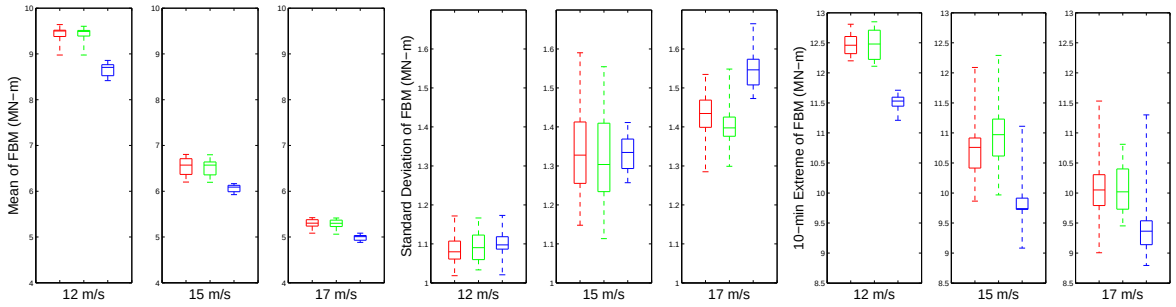

Figure 8. Box-whisker plots summarizing ensemble statistics for FBM based on 15 simulations: mean (left); standard deviation (middle); ten-minute maximum (right).

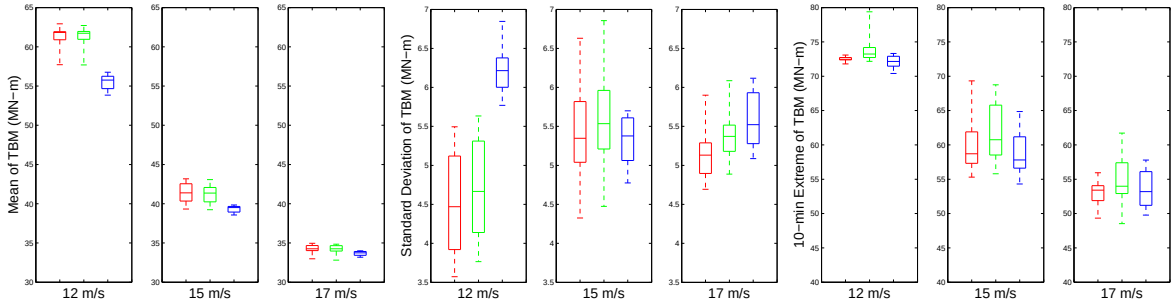

Figure 9. Box-whisker plots summarizing ensemble statistics for TBM based on 15 simulations: mean (left); standard deviation (middle); ten-minute maximum (right).

The loads are seen to have higher standard deviations with increasing wind speed. Ten-minute extreme loads and mean values for the two loads and for the different inflow simulation options suggest that the inflow conditions associated with the hub-height wind speed of 12 m/s bring about the largest loads. These results are understandable since turbine loads generally decrease as wind speeds exceed the rated wind speed due to pitch control actions. In the following discussions, we will focus only on loads from inflow fields with a hub-height mean wind speed of 12 m/s.

B. Power Spectral Density Functions of Turbine Loads

Power spectral densities (PSD) of turbine loads that result from inflow turbulence generated by LES, LES with FIT, and TurbSim are plotted in Figure 10.

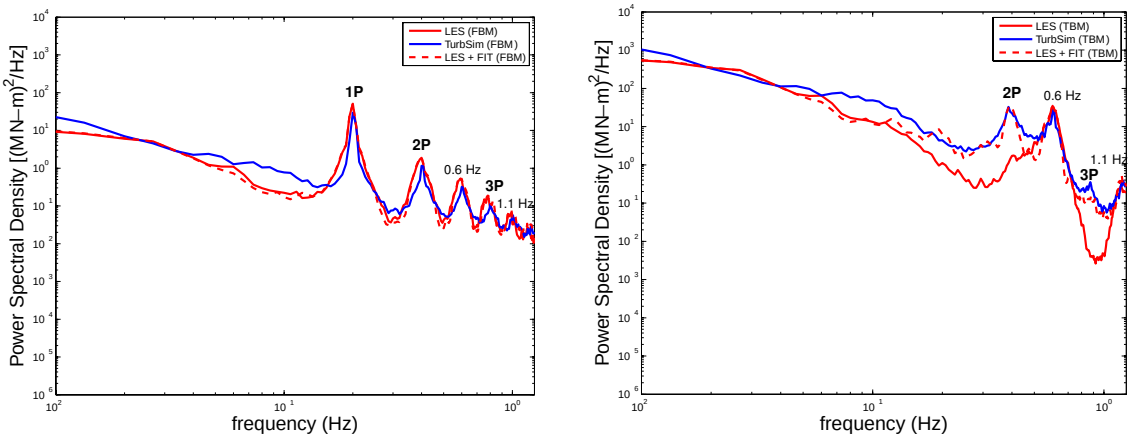

Figure 10. Power spectral density function for FBM (left) and TBM (right) for different inflow simulation options with a hub-height ten-minute mean wind speed of 12 m/s.

The peaks at 0.6 Hz and 1.1 Hz in the spectra match the natural frequencies of the 1^{st} mode of flapwise bending moment and the edgewise bending moment of the blades. On studying the FBM power spectra in Fig. 10, one can see that although there is some energy loss in the PSD for LES and PSD for LES with FIT at low frequencies, the dominant (1P) peak matches that in the PSD for TurbSim quite well, even without applying fractal interpolation. There is slight energy loss at low frequencies but all the peaks shown (such as at 1P, 2P, 3P, etc.) are quite close for all the inflow simulation options.

While the blade loads under inflow turbulence generated by LES preserved the important peaks in the PSDs reasonably well, the TBM power spectrum with LES inflow misses the spectral peak at the natural frequency of the 1^{st} tower fore-aft bending mode at 0.4 Hz (around 2P) as can be seen in Fig. 10. Since this first peak makes an important contribution to the overall energy content, this deficit can lead to errors in tower load estimation. However, fractal interpolation recovers much of the missing energy between 0.4 Hz and 0.8 Hz.

C. Fatigue Load Estimation

Stress range histograms can be established from time series of wind turbine loads by various means including the rainflow cycle counting algorithm,[17] which is a commonly used method used to count the number of cycles in an irregular load or stress time history. Fatigue damage in any single cycle is proportional to the stress range amplitude, S, to the m^{th} power, where m is the Wöhler exponent. In variable-amplitude stress cycles, it is convenient to define an equivalent fatigue load (EFL) which represents the m^{th} root of the expected value of S^m. The expected value of S^m, in turn, is obtained by establishing the empirical distribution of the stress ranges that is achieved by rainflow cycle counting. Note that the EFL measure in combination with the total number of cycles counted is to be interpreted as that derived stress range amplitude (from the variable-amplitude stress history) that causes the same amount of damage as the same number of cycles of a constant-amplitude stress history would.

To obtain equivalent fatigue load (EFL) estimates for the wind turbine, Wöhler exponents equal to 3 and 10, respectively, are assumed for the steel tower (i.e., for TBM) and for the blades composed of fiber composite material (i.e., for FBM).

From each of the 15 simulated time series, load cycles were counted using the rainflow cycle counting algorithm. The counted stress cycles were translated into histograms and the equivalent fatigue load (EFL) and effectve number of cycles (N)was also computed. Figures 11 and 12 show fatigue stress range histograms of FBM and TBM, respectively. Also indicated are EFL and N values.

Stress range histograms based on LES flows are slightly lacking in some of the stress cycle bins compared to the those from the TurbSim flows. It is evident that fractal interpolation helps by filling in some of the missing cycles. Fatigue damage on the blades is somewhat larger for the LES inflow than for the TurbSim inflow. Fractal interpolation, with the additional high-frequency energy, increases the fatigue damage even

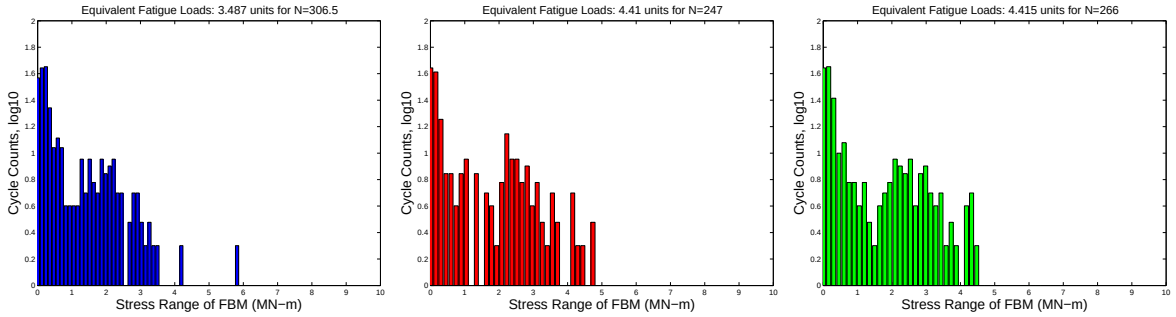

Figure 11. Fatigue stress range histograms based on 15 simulations for FBM (wind speed = 12 m/s): TurbSim (left); LES (middle); LES + FIT (right).

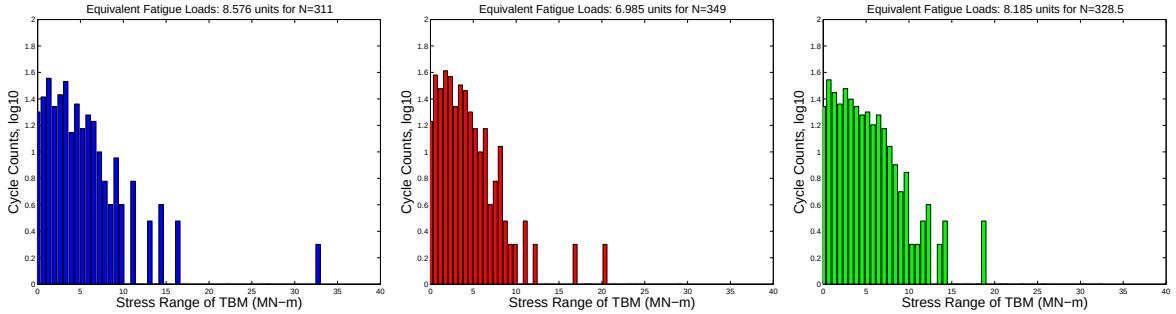

Figure 12. Fatigue stress range histograms based on 15 simulations for TBM (wind speed = 12 m/s): TurbSim (left); LES (middle); LES + FIT (right).

more relative to the TurbSim inflow. However, TBM EFL estimate for LES inflow was about 20% smaller than the EFL value based on TurbSim inflow before FIT was applied; damage was about 40% smaller. After fractal interpolation, the equivalent fatigue load and damage were comparable with that from TubSim inflow, differing by less than 10%.

D. Long-term Load Estimation

The International Electrotechnical Commission (IEC) standard[2] for the design of wind turbines includes a load case (for an ultimate limit state) that requires estimation of a 50-year return period load. In order to estimate this rare load from a limited number of simulations, one needs to use statistical extrapolation to predict this rare long-term load. Design Load Case (DLC) 1.1 in the IEC standard requires inflow turbulence under near-neutral atmospheric conditions and with specified turbulence intensity values that should be simulated with a normal turbulence model (NTM). The ten-minute average hub-height wind speed is treated as a single random variable representing the environment. In addition, to obtain loads for addressing DLC 1.1, the IEC standard requires one to perform aeroelastic simulations for the entire power-producing wind speed range. In this study, our simulations are limited to three specific wind speeds since the objective of this study was only to evaluate alternate inflow simulation methods. As a result, we only compute "short-term" load distributions for the wind speeds studied; we do not attempt a full long-term load extrapolation.

In order to predict short-term load extremes from ten-minute time series, one can use the peak-over-threshold (POT) method or one can extract global (ten-minute) maxima or block maxima (maxima over fixed intervals shorter than ten minutes). Agarwal[18] demonstrated that the three alternative extreme models—peak-over-threshold(POT), global maxima, and block maxima—all give comparable load distributions if a sufficient number of simulations are available to obtain the distribution tails. The present study is based on a limited number of simulations; hence, we use one-minute block maxima to define our extreme load

statistics. Under the assumption that these one-minute maxima are independent of each other, the short-term ten-minute maximum (L) distribution may be obtained for any wind speed $V = v$ from the short-term block maxima (L_{block}). In terms of the probability of exceedance of any load level, l, the short-term global maxima distribution may be expressed as follows:

$$P(L > l | V = v) = 1 - [1 - P(L_{block} > l | V = v)]^n \tag{8}$$

Accounting for the different values of V, the long-term distribution on L can be obtained as follows:

$$P(L > l) = \int_{V_{in}}^{V_{out}} P(L > l | V = v) f_V(v) dv \tag{9}$$

where $f_V(v)$ is the wind speed probability density function which is usually taken to be a Weibull or Rayleigh density function.

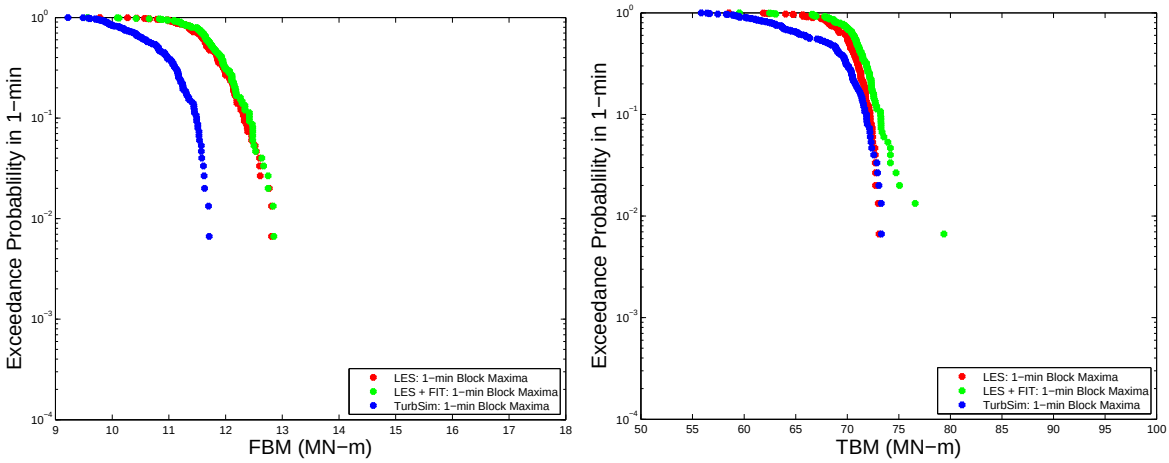

Figure 13. Short-term probability distribution of wind turbine loads for a wind speed of of 12 m/s for FBM (left) and TBM (right).

Figure 13 shows the short-term distribution for FBM and TBM loads. For the FBM loads, fractal interpolation leads to no change in the load distribution obtained using LES. The difference between LES and TurbSim predictions of the 80th percentile ten-minute maximum value (or, equivalently, of the load associated with a 0.022 non-exceedance probability in 1 minute) is approximately 10% for this load. For the TBM loads, the LES distribution matches that from TurbSim while fractal interpolation introduces a deviation in the tail. It appears that excessive high-frequency energy introduced by FIT causes large loads in a few simulations that directly influences the distribution tails. Note, however, that the short-term loads distributions presented here are based only on a limited number of simulations; additional simulations might be warranted to establish stable extreme distribution tails.

V. Conclusions

Turbine loads under inflow turbulence generated by different simulation techniques were compared. Inflow turbulence for a neutrally stable boundary layer generated by conventional stochastic simulation, large-eddy simulation, and large-eddy simulation with fractal interpolation was considered. Load statistics were studied to understand the characteristics of turbine loads at different hub-height wind speeds. The hub-height wind speed of 12 m/s had the largest loads compared to the wind speeds of 15 m/s or 17 m/s. Fractal interpolation was helpful for recovering energy deficit at high frequencies in large-eddy simulations. Fatigue loads and stress range histograms were also studied; again fractal interpolation improves the stress cycle histograms from LES versus stochastic simulation. Short-term load distributions of turbine loads were studied using 1-min block maxima; these distributions from stochastic simulation and LES were reasonably consistent with each other.

Based on the various turbine load studies conducted, it is concluded that large-eddy simulations with fractal interpolation can generate turbine loads that are comparable with the stochastic simulation results. For fatigue and ultimate limit states, LES with FIT is an attractive alternative to stochastic simulation. Having demonstrated its effectiveness as has been done here, future work is planned where LES with FIT will be employed to assess loads on turbines in the stable boundary layer where stochastic simulation is no longer possible.

Acknowledgements

The authors gratefully acknowledge the financial support provided by Sandia National Laboratories (Contract Nos. 681008 and 743358), by the Texas Higher Education Coordinating Boards Norman Hackerman Advanced Research Program (Grant No. 003658-0100-2007), and by the National Science Foundation (Grant Nos. ATM-0748606, CMS-0449128).

References

[1]Jonkman, B., "TurbSim User's Guide: Version 1.50," Tech. Rep. NREL/TP-500-46198, National Renewable Energy Laboratory, Golden, CO, 2009.

[2]International Electrotechnical Commission, Wind Turbines - Part 1: Design Requirements, IEC-61400-1, Edition 3.0, 2007.

[3]Jonkman, J., Butterfield, S., Musial, W., and Scott, G., "Definition of a 5MW Reference Wind Turbine for Offshore System Development," Tech. Rep. NREL/TP-500-38060, National Renewable Energy Laboratory, Golden, CO, 2007.

[4]Jonkman, J. and Buhl, M., "FAST User's Guide," Tech. Rep. NREL/EL-500-38230, National Renewable Energy Laboratory, Golden, CO, 2005.

[5]Hansen, M., *Aerodynamics of Wind Turbines*, Earthscan Publications Ltd., 2nd ed., 2008.

[6]Fogle, J., Agarwal, P., and Manuel, L., "Towards an Improved Understanding of Statistical Extrapolation for Wind Turbine Extreme Loads," *Wind Energy*, Vol. 11, 2008, pp. 613–635.

[7]Kelley, N., Osgood, R., Bialasiewicz, J., and Jakubowski, A., "Using Wavelet Analysis to Assess Turbulence/Rotor Interactions," *Wind Energy*, Vol. 3, 2000, pp. 121–134.

[8]Smagorinsky, J., "General Circulation Experiments with the Primitive Equations," *Monthly Weather Review*, Vol. 91, 1963, pp. 99–164.

[9]Geurts, B., *Elements of Direct and Large-Eddy Simulation*, Edwards, 2003.

[10]Lilly, D., "A Proposed Modification of the Germano Subgrid-scale Closure Method," *Physics of Fluids A*, Vol. 4, 1992, pp. 633–635.

[11]Germano, M., Piomelli, U., Moin, P., and Cabot, W., "A Dynamic Subgrid-scale Eddy Viscosity Model," *Physics of Fluids A*, Vol. 3, 1991, pp. 1760–1765.

[12]Basu, S. and Porté-Agel, F., "Large-Eddy Simulation of Stably Stratified Atmospheric Boundary Layer Turbulence: a Scale-Dependent Dynamic Modeling Approach," *Journal of the Atmospheric Sciences*, Vol. 63, 2006, pp. 2074–2091.

[13]Anderson, W., Basu, S., and Letchford, C., "Comparison of Dynamic Subgrid-scale Models for Simulations of Neutrally Buoyant Shear-driven Atmospheric Boundary Layer Flows," *Enviornmental Fluid Mechanics*, Vol. 7, 2007, pp. 195–215.

[14]Basu, S., Vinuesa, J.-F., and Swift, A., "Dynamic LES Modeling of a Diurnal Cycle," *Journal of Applied Meteorology and Climatology*, Vol. 47, 2008, pp. 1156–1174.

[15]Basu, S., Foufoula-Georgiou, E., and F. Porté-Agel, F., "Synthetic Turbulence, Fractal Interpolation, and Large-Eddy Simulation," *Physical Review E*, Vol. 70, 2004, pp. 026310.

[16]Tukey, J., *Extrapolatory Data Analysis*, New York: Addison-Wesley, 1977.

[17]American Society for Testing and Materials Standards, Standard Practices for Cycle Counting in Fatigue Analysis, E1049-85, 1985.

[18]Agarwal, P., *Structural Reliability of Offshore Wind Turbines*, Ph.D. Dissertation, University of Texas at Austin, 2008.